High-resolution study of (002, 113, 11−1) four-beam diffraction in Si

V. G. Kohn[a]* and A. Kazimirov[b]

[a]National Research Center 'Kurchatov Institute', 123182 Moscow, Russian Federation, and [b]Cornell High Energy Synchrotron Source (CHESS), Cornell University, Ithaca, 14853 New York, USA. Correspondence e-mail: kohnvict@yandex.ru

The results of a high-resolution study of the $(002, 113, 11\bar{1})$ four-beam diffraction in Si are presented. The incident synchrotron radiation beam was highly monochromated and collimated with a multi-crystal arrangement in a dispersive setup in both vertical and horizontal planes, in an attempt to experimentally approach plane-wave incident conditions. The Renninger scheme was used with the forbidden reflection reciprocal-lattice vector 002 normal to the crystal surface. The azimuthal and polar rotations were performed in the crystal surface plane and the vertical plane correspondingly. The polar angular curves for various azimuthal angles were measured and found to be very close to theoretical computer simulations, with only a small deviation from the plane monochromatic wave. The effect of the strong two-beam 002 diffraction was observed for the first time with the maximum reflectivity close to 80%. The structure factor of the 002 reflection in Si was experimentally determined as zero.

1. Introduction

Single crystals of a diamond-type structure (diamond, silicon, germanium) consist of two interpenetrating face-centered cubic sublattices displaced by a quarter of the distance along the cube diagonal. Such a structure leads to the suppression of diffraction with the even–even Miller indices satisfying the condition $h + k + l = 4n + 2$, where n is an integer, for example 002. The suppression occurs as a result of the destructive interference of two waves scattered by different sublattices with opposite signs, or with the phase shift π. The diffraction with Miller indices as the sum of such suppressed indices and the odd–odd allowed indices is also allowed. The suppression is not complete for some indices, for example 222, and complete for other indices, for example 002. Nevertheless, all such indices are called the indices of forbidden reflection by symmetry. Some weak reflection occurs due to the fact that the real electron density in atoms inside the crystal is not fully symmetrical; the same can be said for the displacements of atoms due to thermal vibrations. The diffraction parameter for a weak quasi-forbidden reflection is defined usually as a structure factor F, *i.e.* an effective number of electrons in a unit cell participating in diffraction.

The interesting problem is a search for the means to make such forbidden reflections stronger. The most effective solution is to use multiple diffraction, which takes place at the definite angular position of the crystal where the Bragg condition is met for the forbidden reflection simultaneously with some strong allowed reflections having odd–odd indices. This approach was used for the first time by Renninger (1937),

who proposed a convenient experimental scheme in which the forbidden reflection was normal to the crystal surface, and therefore the Bragg condition was met while the crystal was rotated around the surface normal. Then, at some angles of such rotation (we will call it the azimuthal scan) multiple diffraction takes place when other reflections satisfy the Bragg condition. At these crystal positions the forbidden reflection becomes rather strong and can be reliably detected and studied.

This setup is known as the Renninger scheme and it has been utilized in many multiple-diffraction experiments (see Authier, 2005; Chang, 2004). The main emphasis was given to the possibility of determining the phases of allowed reflections. The first theoretical treatment based on the dynamical theory of *n*-beam diffraction and comparison with the experimental results of the integrated intensities for the case of Ge (222, 113) diffraction was given by Colella (1974). However, all experiments up to the recent time have been performed with the incident beam rather poorly collimated over both the polar and azimuthal angles and therefore the fine details in the angular dependences of the intensities of the beams participating in multiple diffraction have been washed out and lost for analysis.

On the other hand, it was shown by Kohn (1988a) that two successive reflections $000 \rightarrow 113 \rightarrow 222$ can lead to the phenomenon of total reflection of the incident plane wave to the diffracted 222 plane wave at the crystal angular position where the Bragg condition is met well for the 222 forbidden reflection but is met poorly for the 113 allowed reflection. The incident beam must be highly collimated and monochromated

 331

research papers

for experimental recording of the effect of total reflection in the direction of forbidden diffraction. The first attempt at this was by Kazimirov & Kohn (2010). They studied the three-beam (222, 113) case of X-ray diffraction in Si and showed what happens if the incident beam is not collimated and monochromated within the necessary limits. The effect was recorded under the necessary conditions. In the second work of this series (Kazimirov & Kohn, 2011) the three-beam (222, 113) case of X-ray diffraction in Ge was studied in detail under the conditions of rather good collimation and monochromatization. In this work both the central part of the azimuthal scan and the tails were registered. The azimuthal angular dependence of the integrated intensity over a polar angle allowed the authors to obtain the value of the structure factor $F = 1.05$, which turns out to be consistent with the previous studies by Matsushita & Kohra (1974) and Roberto *et al.* (1974).

This work is the third in a series of studies. It presents the results of a high-resolution study of (002, 113, 11$\bar{1}$) four-beam diffraction in Si within the same experimental scheme. The two-beam case 002 is fully forbidden as reported by Tischler *et al.* (1988). On the other hand, the addition of a second reflection 113 leads to excitation of a third reflection 11$\bar{1}$ due to the symmetry of the crystal lattice. While the 002 and 113 beams are Bragg reflected, *i.e.* they are reflected outside the crystal, the 11$\bar{1}$ beam is Laue reflected, *i.e.* inside the crystal. As a result, the polar angular dependences at various azimuthal angles in the central part of the multiple-diffraction region become more complicated. We note that in this experiment an additional effort was made to improve the mechanical stability of the experimental scheme. Accordingly, we obtain very good coincidence between the experimental results and theoretical simulations.

In the next section the theoretical formulae for calculating the multiple diffraction of the incident plane wave are briefly presented; these were used in the computer simulations. In §3 we present the experimental results for the four-beam diffraction angular region together with detailed comparison between these results and computer simulations. Here we also show the two-wave 002 forbidden diffraction integrated intensity as a function of the azimuthal angle near the four-beam diffraction angular region, and discuss the possibility of determining the 002 Si structure factor. §4 contains the conclusions.

2. Theory

The theory of plane-wave multiple diffraction in single crystals was developed in various modifications. The first quasi-exact modification was presented by Colella (1974). In his work the incident plane wave and all diffracted waves are accompanied by mirror waves to satisfy the Maxwell equation with the second derivatives of the electric-field amplitude. Such an approach is usual in optics, but for X-ray crystal optics it is necessary only for the waves moving at a small angle with the crystal surface. Colella reduces the calculation scheme to the $4N \times 4N$ scattering-matrix eigenvalue problem, where N is

the total number of waves. However, it was known from the two-wave dynamical diffraction theory that, if the angles between wave directions and the crystal surface are not small, the mirror waves can be neglected. As a result, the calculation scheme is reduced to the $2N \times 2N$ scattering-matrix eigenvalue problem. Such a formulation of the theory was presented by Kohn (1979) where it was also shown that for a thick crystal the number of permitted modes of the wavefield can be reduced to $2M$, where M is the number of waves directed inside the crystal. The same technique has been proposed by Chang (1979).

Subsequently, Stepanov & Ulyanenkov (1994) have developed the calculation scheme where the mirror waves are taken into account only for the beams with a direction which makes a small angle with the crystal surface. In their approach the calculations are reduced to considering the $2(N + N_s)$ strong wavefields inside the crystal, where N_s is the number of grazing X-ray beams. Such a scheme allows one to obtain the same results as in the Collela scheme but with a considerable gain in the speed and simplicity of the calculations. Stetsko & Chang (1997) discovered an error in the Collela approach which consists of the choice of the unit vectors of the wavefield polarizations independently of the small angular deviation of the incident beam. It is correct for large angles between the beam directions and the crystal surface, but it is wrong for the case of grazing X-ray beams. They propose a new calculation scheme based on the $4N \times 4N$ scattering-matrix eigenvalue problem but in the Cartesian coordinate system. Their approach can also be useful for the two-beam case.

The four-beam case (002, 113, 11$\bar{1}$), considered in this work, does not contain the grazing X-ray beams; therefore we can use the theory developed by Kohn (1979). In this approach we choose the unit vectors of two polarization states $s = \pi, \sigma$ for the electric-field direction of the incident and all diffracted waves. Then, the normalized reflection powers for the Bragg-diffracted beams, which leave the crystal plate through the same side where the incident beam enters the crystal, can be calculated as follows:

$$R_m^{(s)}(\theta, \varphi) = \sum_{s'} \left| \sum_j B_{ms'}(j) \, c_s(j) \right|^2. \tag{1}$$

Here the index m indicates the beams ($m = 0$ for the incident beam), the index j is used to distinguish various Bloch waves or zones of the dispersion surface, and the parameters $c_s(j)$ determine the rate of excitation of the jth Bloch wave. The summation is performed over the values which correspond to the positive value of the absorption coefficient $\mu_j = \mathrm{Im}(\varepsilon_j)$.

The complex Bloch-wave amplitudes $B_{ms}(j)$ and the complex dispersion parameters ε_j are the solution of the eigenvalue problem

$$\sum_{ns'} G_{mn}^{ss'}(\theta, \varphi) B_{ns'}(j) = \varepsilon_j B_{ms}(j), \tag{2}$$

where the scattering matrix G is determined as

$$G_{mn}^{ss'}(\theta, \varphi) = \frac{2\pi \chi_{mn}}{\lambda \gamma_m^{1/2} \gamma_n^{1/2}} (\mathbf{e}_{ms} \mathbf{e}_{ns'}) - \alpha_m(\theta, \varphi) \delta_{mn}^{ss'}. \tag{3}$$

Here $\mathbf{e}_{ms}$ are the unit polarization vectors for the wave m, λ is the wavelength of X-ray radiation, γ_m is the cosine of the angle between the direction of the mth beam and the internal normal to the entrance surface, χ_{mn} is the Fourier image of the complex polarizability of the crystal with the reciprocal-lattice vector $\mathbf{h}_m - \mathbf{h}_n$, $\delta_{mn}^{ss'}$ is the Kroneker's symbol, and

$$\alpha_m(\theta, \varphi) = \frac{2}{\gamma_m}\left[(\mathbf{h}_m\mathbf{e}_1)\Delta\theta + (\mathbf{h}_m\mathbf{e}_2)\Delta\varphi - (\mathbf{h}_m\mathbf{s}_0)\frac{\Delta\lambda}{\lambda}\right], \quad (4)$$

where $\Delta\theta = \theta - \theta_B$ and $\Delta\varphi = \varphi - \varphi_0$ mean the angular deviations of the incident-beam direction from the direction of kinematical multiple diffraction, i.e. without accounting for refraction of waves inside the crystal. The unit vectors $\mathbf{e}_1$ and $\mathbf{e}_2$ are normal to the incident-beam direction $\mathbf{s}_0$. We choose $\mathbf{e}_1$ to be in the scattering plane for the forbidden reflection ($m = 1$), so $\mathbf{e}_2$ is normal to this plane. As was shown by Kohn (1979), in a thick crystal the parameters $c_s(j) = 0$ if j indicates the Bloch wave with $\mu_j < 0$. The remaining values may be found from the linear set of equations

$$\sum_j B_{ms'}(j)c_{s'}(j) = \delta_{m0}^{ss'} \quad (5)$$

where the index m runs only over the Laue beams with $\gamma_m > 0$.

Equations (1)–(5) were used in this work for computer simulations of the experimental results and detailed comparison between the theoretical and experimental curves. We are interested mainly in the first 002 beam ($m = 1$), which we will treat as a quasi-forbidden, i.e. we shall assume the existence of a small structure factor F due to asymmetry of the electron density; therefore $\chi_{10} \neq 0$. Considering the plane of angular deviations ($\Delta\theta, \Delta\varphi$) as they are determined here, we obtain that the Bragg condition for wave 1 is met along the vertical line, i.e. independently of $\Delta\varphi$. This line corresponds to the azimuthal scan and there are three regions on this line. We define the first region as one where wave 1 has a large amplitude together with wave 2. In the second region wave 1 has a large amplitude alone, and the third region is the tails where the two-beam case with wave 1 is realized, and the amplitude of the diffracted wave is very small or zero.

The second region is the most interesting, because here the effect of total reflection in the forbidden direction was predicted theoretically by Kohn (1988a) and observed experimentally by Kazimirov & Kohn (2010, 2011). To illustrate the effect analytically we simplify the problem and consider hard radiation when the Bragg angles are small. In this case one can choose the polarization vectors in such a way that all π vectors are approximately parallel to each other and normal to all σ vectors. Then the general eightfold system can be divided into two fourfold systems of equations and the index s can be omitted. We have strong B_0 and B_1 amplitudes but small B_2 and B_3 amplitudes. Also we have small $\Delta\theta$ and relatively large $\Delta\varphi$.

Then, the small amplitudes B_n, $n = 2, 3$, can be calculated by means of the perturbation method from equation (2) as

$$B_n = \frac{G_{n0}B_0 + G_{n1}B_1}{[\varepsilon - G_{nn}(\Delta\varphi)]}. \quad (6)$$

Substitution of these equations into two other equations leads to the system of the quasi-two-beam case for the strong amplitudes B_0 and B_1, namely,

$$g_{00}B_0 + g_{01}B_1 = \varepsilon B_0$$
$$g_{10}B_0 + g_{11}B_1 = \varepsilon B_1. \quad (7)$$

The effective matrix of this system is as follows ($m, n = 0, 1$):

$$g_{mn} = G_{mn} + \frac{D_{mn}}{\Delta\varphi}, \quad D_{mn} = \sum_{k=2,3} D_{mnk}, \quad (8)$$

where

$$D_{mnk} = \frac{\gamma_k G_{mk}G_{kn}}{2(\mathbf{h}_k\mathbf{e}_2)}. \quad (9)$$

Here we replaced the denominator $\varepsilon - G_{kk}(\Delta\varphi)$ by the value $-\alpha_k(\Delta\varphi) = [2(\mathbf{h}_k\mathbf{e}_2)/\gamma_k]\Delta\varphi$ because these equations are written for the case of rather large values of $\Delta\varphi$ and we consider small values of ε. Equations (7) and (8), in a more general case and with taking into account polarizations, were obtained for the first time by Høier & Marthinsen (1983) as a method of approximate numerical solution of the multiple-diffraction problem. However, we perform the numerical solution accurately.

The properties of two-beam diffraction are well known. It was shown by Kazimirov & Kohn (2010) that assuming a symmetrical case ($\gamma_1 = -\gamma_0$) we have

$$\varepsilon = g_{00} + (-g_{01}g_{10})^{1/2}[-y \pm (y^2 - 1)^{1/2}], \quad (10)$$

where

$$y = \frac{g_{00} - g_{11}}{2(-g_{01}g_{10})^{1/2}} = \frac{\Delta\theta - \theta_0}{\theta_1}, \quad \theta_1 = \frac{\lambda(-g_{01}g_{10})^{1/2}}{4\pi\cos\theta_B} \quad (11)$$

$$\theta_0 = -\frac{\chi_0}{\sin(2\theta_B)} + \frac{C_0}{\Delta\varphi}, \quad C_0 = \frac{\lambda(D_{11} - D_{00})}{8\pi\cos\theta_B}. \quad (12)$$

The center of the reflectivity maximum corresponds to the condition $y = 0$, i.e. $\Delta\theta = \theta_0$, while the width of the region of the reflectivity maximum is defined from the condition $|y| < 1$. In a scale of $\Delta\theta$ the center is shifted permanently owing to a refraction of the waves at the crystal surface. In addition, there is a variable shift due to interaction with weak diffracted waves, which is asymmetrically dependent on $(\Delta\varphi)^{-1}$. If the diffraction is pure forbidden, then the width of the region of the reflectivity maximum $2\theta_1$ depends symmetrically on $|\Delta\varphi|^{-1}$. However, if the diffraction is quasi-forbidden one has to observe asymmetrical dependence. We note that this width is inversely proportional to the depth of reflection inside the crystal. If such a depth becomes larger than the penetration depth due to absorption, the maximum value decreases and becomes significantly less than unity.

3. Experiment and fit

The experiment was performed at the Cornell High Energy Synchrotron Source (CHESS) at the A2 beamline. The X-ray beam from the 49-pole wiggler was monochromated
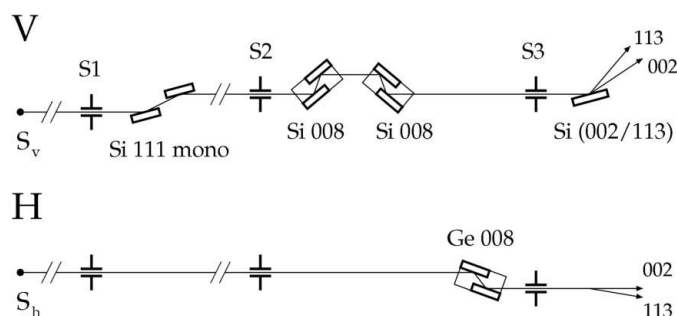
Figure 1
Experimental setup. In the vertical diffraction plane (upper panel) two Si 008 channel-cut crystals in the dispersive setup were used for the main monochromatization and angular collimation. In the horizontal diffraction plane (lower panel) the beam was collimated with the Ge 008 channel-cut crystal.

Figure 2
Three-dimensional picture of the beam directions together with the rotation axes' directions and the crystal plate.

to the photon energy 20.492 keV with a standard double-crystal Si 111 upstream water-cooled monochromator. Post-monochromator optics for the main monochromatization and angular collimation were assembled on the optical table in the experimental hutch. The sample, a thick Si (001)-oriented perfect crystal, was mounted on a Huber four-circle diffractometer. The measurements were performed at the ambient temperature in the hutch of 295 ± 1 K. The diffraction plane for the forbidden 002 reflection was vertical. The intensities of the 002 and 113 Bragg-reflected beams were recorded as a function of the polar angle θ for various values of the azimuthal angle φ in the vicinity of the four-beam (002, 113, $11\bar{1}$) diffraction.

The experimental setup is shown schematically in Fig. 1. Two diffraction planes, vertical (V) and horizontal (H), are shown on separate panels. The main monochromatization and collimation over the polar angle were performed with two Si 008 channel-cut crystals in a dispersive arrangement. The azimuthal angular collimation was achieved with a double-bounce Ge 008 channel-cut crystal diffracting in the horizontal plane. To perform scans with sub-μrad angular steps additional gear boxes were added to standard Huber gear reducers on both θ and φ axes. In this experiment the new sample shifter was used. The motion was fulfilled with four piezoelectric crystals, each of them having a precision sensor of shift. The program that controls the experiment interacts with the controller, which is itself a computer. It sends signals (voltage) on the piezoelectric crystals and reads the sensor data. In this way a correction of shift was performed over the full duration of the experiment.

The $11\bar{1}$ beam was directed inside the crystal and was fully absorbed in it. Therefore this beam is not registered. Nevertheless, the existence of this beam can be seen in the change of reflection of the other beams. The three-dimensional picture of the beam directions together with the crystal orientation and rotational axes is shown in Fig. 2. We note that, even for relatively small values of the azimuthal angle, the distance between polar angles satisfying the Bragg condition for beams 002 or 113 and for beam $11\bar{1}$ becomes rather large. Therefore the existence of the fourth beam is essential only for the
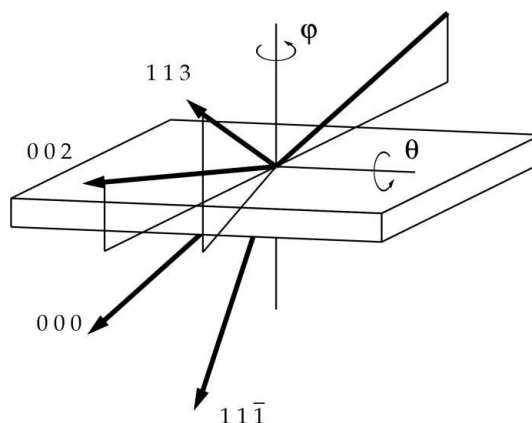
central region of four-beam diffraction. With increasing azimuthal angle deviation from the center the behavior of the polar angular dependence soon becomes similar to the case of the three-beam (002, 113) diffraction.

Fig. 3 shows 12 reflectivity curves of the polar ($\Delta\theta$) dependence for both 002 and 113 beams for various values of the azimuthal angle deviation $\Delta\varphi$. The values of $\Delta\varphi$ are shown inside the panels. The two first and two last $\Delta\varphi$ values can be referred to as the second azimuthal scan region. All other panels correspond to the first region, where two reflected waves have simultaneously large intensity. The solid lines show the theoretical simulations, the circles show the experimental values for the 002 beam, the rectangles show the experimental results for the 113 beam. The computer simulation curves are shown exactly. As for the experimental results, it is very difficult to perform exact normalization of the data, as well as to determine the origin on the angular scale. Therefore these parameters are considered as free and their values were determined from the best fit.

It is easy to see that the panels of the second azimuthal scan region (the two first and two last) are similar to the three-beam case. The regions of two-beam total reflection for the 002 and 113 beams are located at different places and do not intersect. The location of region for the 113 beam moves from the right to the left. As for the location of region for the 002 beam, it is approximately the same. However, some asymmetric deviation from the middle value can be seen. The center of the 002 peak is equal to $\Delta\theta = 9$ μrad for $\Delta\varphi = -16.5$ μrad, and $\Delta\theta = 11$ μrad for $\Delta\varphi = 20$ μrad. As in the three-beam case considered by Kazimirov & Kohn (2010) there is some additional peak of another beam inside the region of strong reflection of each beam. This additional peak is generated by both the incident beam and strongly reflected beam and has an asymmetric shape owing to the change of the phase difference between the complex amplitudes of the incident and strongly reflected beams. Such a shape is characteristic of the curve of the yield of secondary radiation in the standing-wave technique (Kovalchuk & Kohn, 1986a,b) and was described for the first time by Kohn (1988b).
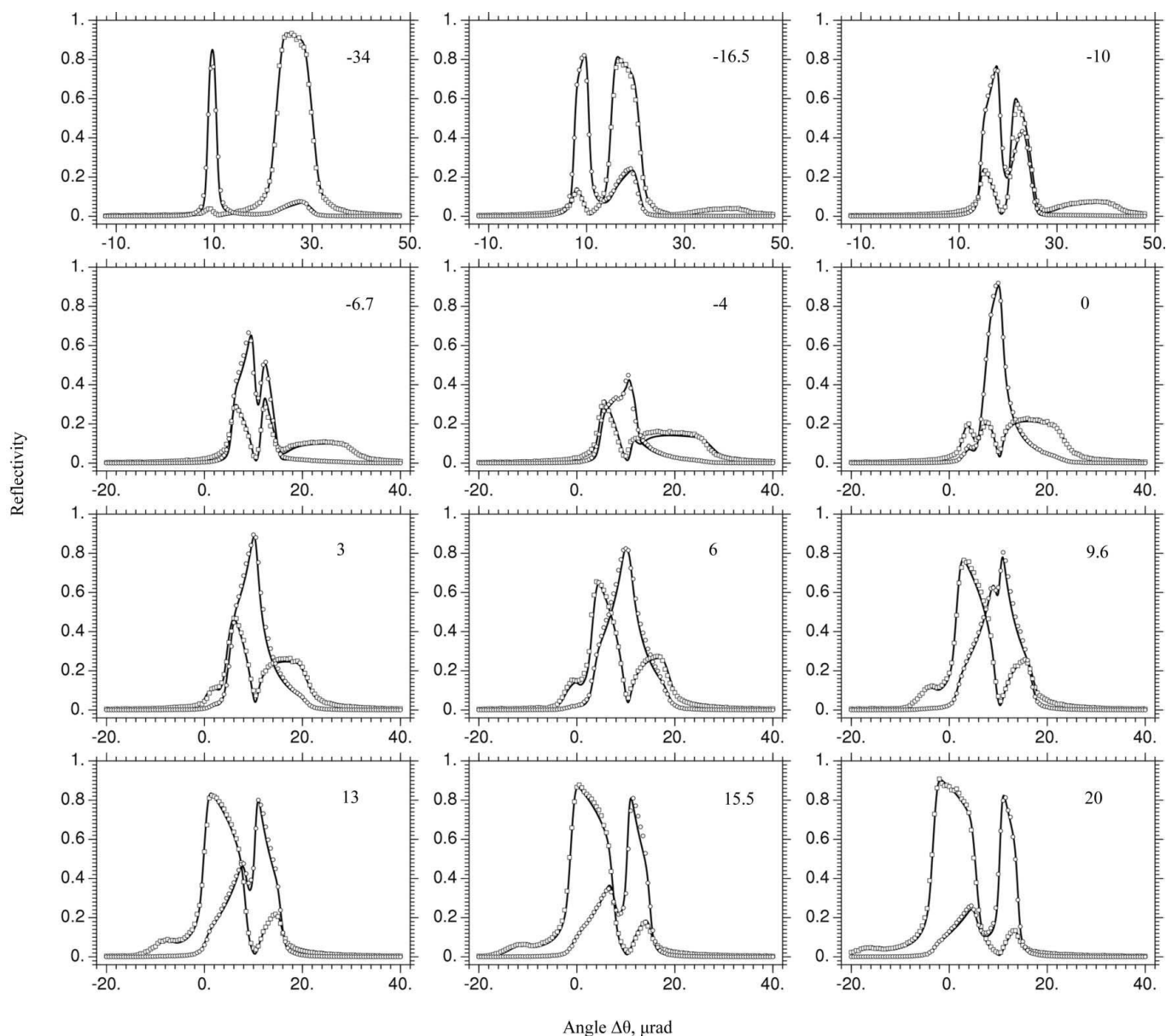
Figure 3
Theoretical and experimental polar (θ) 002 and 113 diffraction profiles. Azimuthal (φ) angles for each curve are shown inside the panels. Solid line – theory, circular markers – 002 experiment, rectangular markers – 113 experiment.

The existence of the fourth $11\bar{1}$ wave can be seen in the panels for $\Delta\varphi = -6.7$, -4 and 0 µrad as an additional peak on the intensity curve for the 113 wave at the right-hand side. Inside this region the Bragg condition for the 113 wave is not fulfilled, but it is fulfilled for the $11\bar{1}$ wave. As a result the double diffraction $000 \rightarrow 11\bar{1} \rightarrow 113$ takes place. The asymmetrical shape of the additional peak is not observed because the wave $11\bar{1}$ is reflected inside the crystal. In the panels for $\Delta\varphi = 3$, 6, 9.6 and 13 µrad the additional $11\bar{1}$ wave is the reason for the more complicated shape of the curves compared to the three-wave case. It is of interest that the peculiarity of the (222, 113) three-wave case consisting of a zero value of the 113 wave intensity at the point of the exact Bragg condition for the forbidden diffracted wave can be seen in this case too.

Now equation (2) without polarizations can be written as

$$\begin{pmatrix} G_{00} & 0 & G_{02} & G_{03} \\ 0 & G_{11} & G_{12} & G_{13} \\ G_{20} & G_{21} & G_{22} & G_{23} \\ G_{30} & G_{31} & G_{32} & G_{33} \end{pmatrix} \begin{pmatrix} B_0 \\ B_1 \\ B_2 \\ B_3 \end{pmatrix} = \varepsilon \begin{pmatrix} B_0 \\ B_1 \\ B_2 \\ B_3 \end{pmatrix}. \quad (13)$$

In our specific case we have the additional relations $G_{30} = G_{21}$, $G_{20} = G_{31}$. Of course, if the Bragg condition is not fulfilled for beam 3, *i.e.* $|G_{33}/G_{00}| \gg 1$, we can neglect the fourth equation and use $B_3 = 0$ in the first three equations. Then we obtain the solution with $\varepsilon = G_{00}$, $B_1 = -G_{20}B_0/G_{21}$ and $B_2 = 0$ in the angular point where $G_{11} = G_{00}$. The last condition just means the Bragg condition for beam 1. In the central part where the relation $|G_{33}/G_{00}| \gg 1$ is not fulfilled the same solution can be obtained under the additional
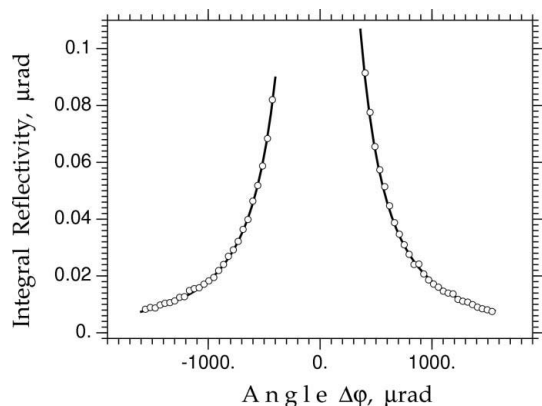
Kohn and Kazimirov · Study of (002, 113, 11−1) diffraction in Si **335**

Figure 4
Theoretical and experimental 002 φ azimuthal curve of integral intensity over polar angle. Solid line – theory, circular markers – 002 experiment.

condition $G_{20}^2 = G_{21}^2$. Since this condition is not completely met, the pit of 113 wave intensity is not zero but rather small.

We note also that the additional $11\bar{1}$ wave influences the 113 wave more strongly than the forbidden 002 wave. However, in the panel for $\Delta\varphi = -4$ µrad both waves become very different from the case of three-wave diffraction. A detailed physical analysis of the reasons for such behavior of the intensity curves lies out of the scope of this work. The main goal was to obtain the best coincidence between the theory and the experiment. This goal was achieved. We note that the theoretical curves were averaged over the 3 µrad region of the azimuthal angle $\Delta\varphi$. Also the convolution of theoretical curves with the Gaussian function with 0.8 µrad FWHM was used. These are approximately the same parameters that we used in the previous works.

All calculations were performed under the assumption that the diffraction 002 is strictly forbidden, *i.e.* the structure factor $F = 0$. This value was reported by Tischler *et al.* (1988). To confirm this conclusion we have measured the polar dependence of the intensity of the forbidden wave 002 for large values of the azimuthal angle $\Delta\varphi$. All curves have the shape of a two-beam peak like a Gaussian curve with decreasing maximum value and the width of the peak. Then we performed a fit of the integral reflectivity over the polar angle values with the calculations. The results appear as tails of the azimuthal dependence of the integral reflectivity, as shown in Fig. 4. The vertical scale corresponds to the calculated value, and the normalization of the experimental values was performed from the condition of the best fit. If F is not zero, then the tails must be asymmetrical with a minimum value on one side. However, the experimental results show fully symmetrical dependence which completely coincides with the calculations.

4. Conclusion

The forbidden reflection 002 was excited by means of four-beam (002, 133, $11\bar{1}$) diffraction in Si for the first time. The highly monochromated and collimated incident beam allows us to measure almost plane-wave reflectivity curves of polar angular dependence for various values of the azimuthal angle. Taking into account the parameters of the incident beam in theoretical calculations we demonstrate for the first time excellent coincidence between the results of theory and experiment. Although the beam $11\bar{1}$ is directed into the crystal plate and fully absorbed, it influences significantly the reflectivity of the 113 beam, but not so much the reflectivity of the forbidden 002 beam. An almost two-beam reflectivity curve was measured for the forbidden reflection 002 with the maximum reflectivity up to 80%. The width of such a curve depends on the value of the azimuthal angle $\Delta\varphi$ and can be made as small as necessary by simply rotating the crystal. The 002 case is better than the 222 case for use as a new kind of monochromator with a variable reflectivity band because the two-beam structure factor is equal to zero.

References

Authier, A. (2005). *Dynamical Theory of X-ray Diffraction*, 3rd ed. Oxford University Press.
Chang, S.-L. (1979). *Acta Cryst.* A**35**, 543–547.
Chang, S.-L. (2004). *X-ray Multiple-Wave Diffraction: Theory and Application*. Springer Series in Solid-State Sciences. Berlin: Springer.
Colella, R. (1974). *Acta Cryst.* A**30**, 413–423.
Høier, R. & Marthinsen, K. (1983). *Acta Cryst.* A**39**, 854–860.
Kazimirov, A. & Kohn, V. G. (2010). *Acta Cryst.* A**66**, 451–457.
Kazimirov, A. & Kohn, V. G. (2011). *Acta Cryst.* A**67**, 409–414.
Kohn, V. G. (1979). *Phys. Status Solidi A*, **54**, 375–384.
Kohn, V. G. (1988*a*). *Kristallografiya*, **33**, 567–573.
Kohn, V. G. (1988*b*). *Phys. Status Solidi A*, **106**, 31–39.
Kovalchuk, M. V. & Kohn, V. G. (1986*a*). *Usp. Fiz. Nauk*, **149**, 69–103.
Kovalchuk, M. V. & Kohn, V. G. (1986*b*). *Sov. Phys. Usp.* **29**, 426–446.
Matsushita, T. & Kohra, K. (1974). *Phys. Status Solidi*, **24**, 531–541.
Renninger, M. (1937). *Z. Naturwiss.* **25**, 43.
Roberto, J. B., Batterman, W. & Keating, D. T. (1974). *Phys. Rev. B*, **9**, 2590–2599.
Stepanov, S. A. & Ulyanenkov, A. P. (1994). *Acta Cryst.* A**50**, 579–585.
Stetsko, Yu. P. & Chang, S.-L. (1997). *Acta Cryst.* A**53**, 28–34.
Tischler, J. Z., Budai, J. D., Ice, G. E. & Habenschuss, A. (1988). *Acta Cryst.* A**44**, 22–25.